CHEMISTRY
A EUROPEAN JOURNAL

DOI: 10.1002/chem.200500371

VIP

A Photoactive Molecular Triad as a Nanoscale Power Supply for a Supramolecular Machine

Sourav Saha, Erik Johansson, Amar H. Flood, Hsian-Rong Tseng, Jeffrey I. Zink,* and J. Fraser Stoddart*[a]

Abstract: A tetrathiafulvalene–porphyrin–fullerene (TTF–P–C_{60}) molecular triad, which generates electrical current by harnessing light energy when self-assembled onto gold electrodes, has been developed. The triad, composed of three unique electroactive components, namely, 1) an electron-donating TTF unit, 2) a chromophoric porphyrin unit, and 3) an electron-accepting C_{60} unit, has been synthesized in a modular fashion. A disulfide-based anchoring group was tagged to the TTF end of the molecule in order to allow its self-assembly on gold surfaces. The surface coverage by the triad in a self-assembled monolayer (SAM) was estimated to be 1.4 nm^2 per molecule, a density which is consistent with hexagonal close-packing of the spherical C_{60} component (diameter ~1 nm). In a closed electronic circuit, a triad-SAM functionalized working-electrode generates a switchable photocurrent of ~1.5 $\mu A\,cm^{-2}$ when irradiated with a 413 nm Kr-ion laser, a wavelength which is close to the porphyrin chromophore's absorption maximum peak at 420 nm. The electrical energy generated by the triad at the expense of the light energy is ultimately exploited to drive a supramolecular machine in the form of a [2]pseudorotaxane comprised of a π-electron-deficient tetracationic cyclobis(paraquat-*p*-phenylene) ($CBPQT^{4+}$) cyclophane and a π-electron-rich 1,5-bis[(2-hydroxyethoxy) ethoxy]naphthalene (BHEEN) thread. The redox-induced dethreading of the $CBPQT^{4+}$ cyclophane from the BHEEN thread can be monitored by measuring the increase in the fluorescence intensity of the BHEEN unit. A gradual increase in the fluorescence intensity of the BHEEN unit concomitant with the photocurrent generation, even at a potential (0 V) much lower than that required (−300 mV) for the direct reduction of the $CBPQT^{4+}$ unit, confirms that the dethreading process is driven by the photocurrent generated by the triad-SAM.

Keywords: actuation · electron transfer · fluorescence · photocurrents · pseudorotaxanes

Introduction

Molecular recognition and self-assembly processes are now being harnessed[1] under the umbrella of template-directed synthesis to produce active supramolecular and molecular components in the rapidly evolving fields of nanoelectronics[2] and nanoelectromechanical systems (NEMS),[3] because of their interesting stereoelectronic and mechanical properties[4] that are tunable even at a nanoscale level. Pseudorotaxanes[5] and bistable rotaxanes[6] are amongst some of the best-qualified candidates for the active supramolecular or molecular components of artificial molecular machines[7,8] in fully integrated electronic circuitry. The structural uniqueness of interlocked molecules involving two or more noncovalently bound components allow us to organize, power, and control their actuation at the molecular level in devices by employing external stimuli, such as those provided by chemical, electrochemical, and photochemical inputs. To maintain size and dimension, nanoscale machinery requires a nanoscale power supply. As a means of incorporating a source of electrical energy directly into molecular mechanical systems, we have studied a photoactive donor–chromophore–acceptor molecular triad[9,10] that mimics[11] the photosynthetic energy transduction process by harnessing light energy to generate electrical current. In this program of research, we have demonstrated that the photoactive molecular triad **1**, whose structural formula is revealed in Figure 1a, can generate electrical energy at the expense of light energy, the wavelength of which has been tuned specifically to the ab-

[a] S. Saha, E. Johansson, Dr. A. H. Flood, Dr. H.-R. Tseng, Prof. J. I. Zink, Prof. J. F. Stoddart
The California NanoSystems Institute and
Department of Chemistry and Biochemistry
University of California, Los Angeles
405 Hilgard Avenue, Los Angeles, CA 90095–1569 (USA)
Fax:(+1) 310-206-1843
E-mail: zink@chem.ucla.edu
stoddart@chem.ucla.edu

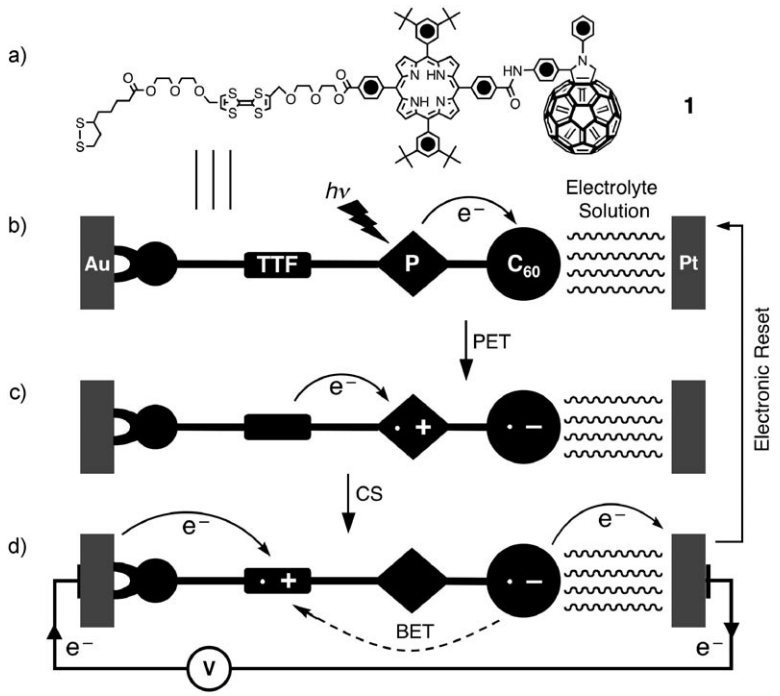

Figure 1. a) The structural formula of the tetrathiafulvalene-porphyrin-fullerene molecular triad **1** bearing a disulfide anchoring group to enable the formation of a SAM on gold (Au). The triad **1**-SAM was employed in a photoelectrochemical cell to demonstrate the generation of electrical energy from light. b)–d) Proposed vectorial electron transfer mechanism for the photo-response of a photoelectrochemical cell comprised of a SAM of the triad **1** on an Au electrode in contact with an electrolyte solution that contains a platinum (Pt) counter electrode (reference electrode not shown) connected externally to a potentiostat (PET = photoinduced electron transfer; CS = charge shift; BET = back-electron transfer).

sorption maxima of the chromophoric unit. Finally, this molecular power supply was employed to drive a supramolecular machine, in the form of a donor–acceptor pseudorotaxane.[5]

A lot of effort has been devoted[9–11] to developing a variety of donor–chromophore–acceptor-based molecular triads that are capable of intramolecular photoinduced electron transfer (PET) from the donor to the acceptor unit. The photogenerated charge-separated states of two classes of such molecular triads have already been demonstrated to generate[9] electrical currents in closed electrical circuits and to enable active transportation[11] of protons and Ca^{2+} ions across artificial lipid membranes. The best known of the fullerenes, namely C_{60}, is one of the most potent electron acceptors,[9c] because of its three-dimensional spherical geometry that supports very low electronic reorganization energy, which, in turn, sustains a long-lived and stable charge-separated state. Porphyrins (P) are often employed[9–12] as universal and efficient chromophores. In a donor–chromophore–acceptor-based triad constitution, a PET from the porphyrin's singlet excited state to the C_{60} unit, followed by a charge shift (CS) to the donor unit, leads ultimately to a relatively stable charge-separated intermediate ($D^{\cdot+}$–P–$C_{60}^{\cdot-}$).[9] The resulting charge-separated state is actually responsible for the generation of a photocurrent on account of a unidirectional electron flow from a functionalized working electrode, through a light-harvesting triad, to a counter electrode through an electrolyte solution in a complete electronic circuit. Molecular triads involving tetrathiafulvalene (TTF) and π-extended TTF components are already known to produce long-lived (μs) charge-separated states.[10] This background provided us with the impetus to introduce TTF as the donor unit into our triad design. Electronic reset by back-electron transfer (BET) within the charge-separated species and/or a unidirectional electron flow in a closed circuit restores the neutral ground state of the triads.

We report here the design and modular synthesis of a TTF–P–C_{60} based molecular triad **1** and how it generates (Figure 1b–d) electrical energy by harnessing light energy. By attaching a disulfide-based, terminal anchoring group, the triad **1** can be self-assembled onto gold electrode surfaces. The modular approach adopted for synthesis could be exploited to fine-tune the electronic properties—namely, the lifetime of the charge-separated intermediates, redox charges, and so forth—according to Marcus–Hush theory by subsequent structure-property feedback loops. In the triad **1** constitution, a diethylene glycol spacer unit was incorporated between the TTF and porphyrin units in order to separate the donor and acceptor units. Finally, this nanoscale source of electrical energy was utilized[13] to drive[5] the dethreading of a supramolecular machine in the form of a [2]pseudorotaxane composed of the π-electron-accepting cyclobis(paraquat-*p*-phenylene) ($CBPQT^{4+}$) cyclophane complexed with the π-donating 1,5-bis[(2-hydroxyethoxy)ethoxy]naphthalene (BHEEN).

Results and Discussion

Synthesis: A modular approach was adopted (Scheme 1) for the overall synthesis of the molecular triad **1**. The key precursors were prepared separately from commercially available starting materials and were subsequently attached together to build up the dyad, and then finally, the triad **1**. The modularity in the synthetic approach is dependent upon the generation of three individual components—namely, 1) an electron-accepting C_{60} unit, 2) a chromophoric porphyrin unit, and 3) an electron-donating TTF unit, all having unique electronic and chemical properties—with ease and

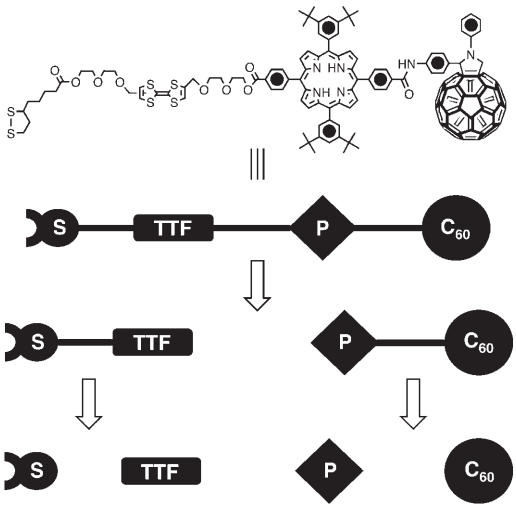

Scheme 1. Retrosynthetic approach of the triad **1**.

simplicity by following known synthetic protocols. Scheme 2 outlines the synthesis of the C_{60} unit. To begin with, C_{60} was functionalized by a 1,3-dipolar cycloaddition[14] of *N*-phenylglycine (**2**) and the *N*-boc-protected derivative **3** of 4-aminobenzaldehyde.[15] Deprotection provided the C_{60} derivative **5**, bearing a reactive amino group. Scheme 3 outlines the synthesis of the porphyrin unit. The C_2-symmetric *meso*-porphyrin **7** was synthesized by using an acid-catalyzed cyclization[16] of 3,5-di-*tert*-butylbenzaldehyde with the bispyrrole **6**, which had been obtained previously by an acid-catalyzed reaction[16] of pyrrole with methyl 4-formylbenzoate. Saponification of the methyl ester functions afforded the corresponding porphyrin–dicarboxylic acid **8**. One of the two carboxylic acid groups in **8** was protected as its benzyl ester in the presence of *N*-methylmorpholine, by using the activating agents, 2-chloro-4,6-dimethoxy-1,3,5-triazine and 4-dimethylaminopyridine (DMAP), to generate the key porphyrin precursor **9**. Scheme 4 outlines the synthesis of the TTF unit. The TTF diester **10** was prepared by Michael additions of intermediate sulfur ylides to methylpropiolate.[17] A diisobutyl aluminum hydride (DIBAL-H)-mediated reduction of the diester **10** to the corresponding diol **11**,[17] followed by a dialkylation of **11** with the protected iodide **13**,[18] furnished the modified TTF-diol **14**. Esterification of one of the terminal primary hydroxyl groups in **14** with thioctic acid afforded the alcohol **15**.

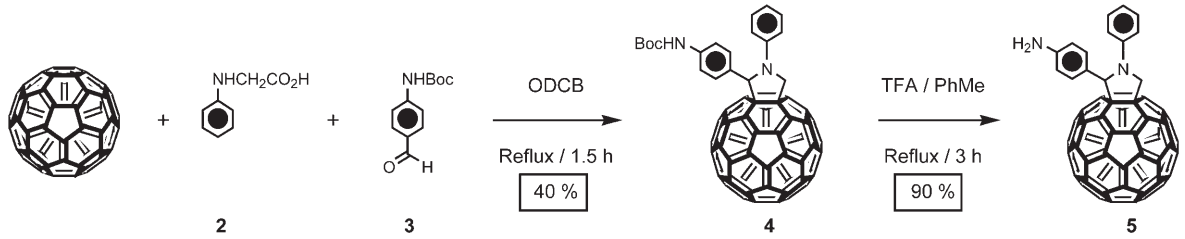

Scheme 2. The preparation of the C_{60} component **5**.

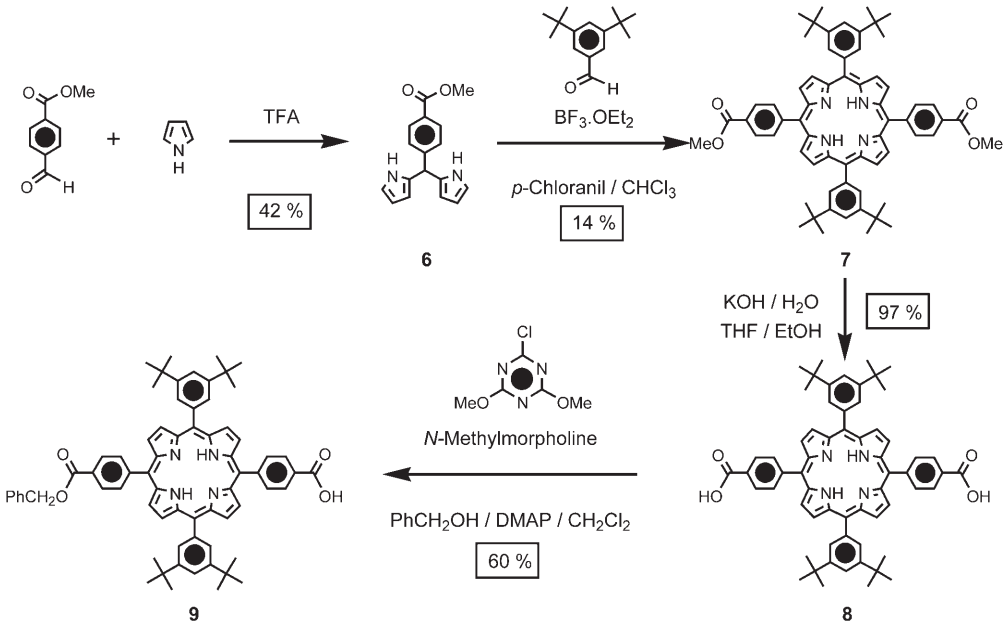

Scheme 3. The preparation of the porphyrin component **9**.

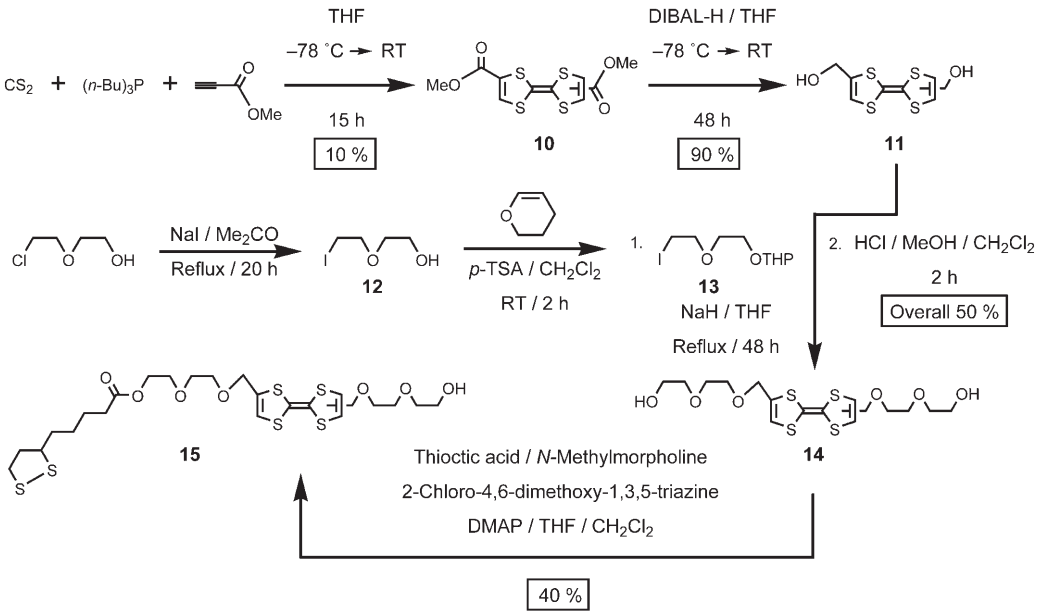

Scheme 4. The preparation of the TTF component **15**.

The manner in which the three pieces—namely, **5**, **9**, and **15**—were brought together to form the triad **1** is illustrated in Scheme 5. The amine-appended C_{60} derivative **5** was subjected to an amide bond-forming reaction with the porphyrin derivative **9** in the presence of 2-chloro-4,6-dimethoxy-1,3,5-triazine as the coupling reagent to form the P–C_{60} dyad **16**. BBr_3-mediated deprotection[10b] of the benzyl ester provided the P–C_{60} dyad **17** containing a free carboxyl group. Finally, an esterification[10b] of this dyad **17** with the alcohol **15**, by using the same coupling conditions, afforded the target triad **1**. This triad, as well as the dyads **16** and **17**, and the alcohol **15**, and all their precursors were characterized by mass spectrometry and ^{1}H NMR spectroscopy.

The triad **1**, which contains a terminal disulfide-anchoring group, was self-assembled on gold wires and foils by immersing them in 0.1 mM solutions of the triad in dichloro-

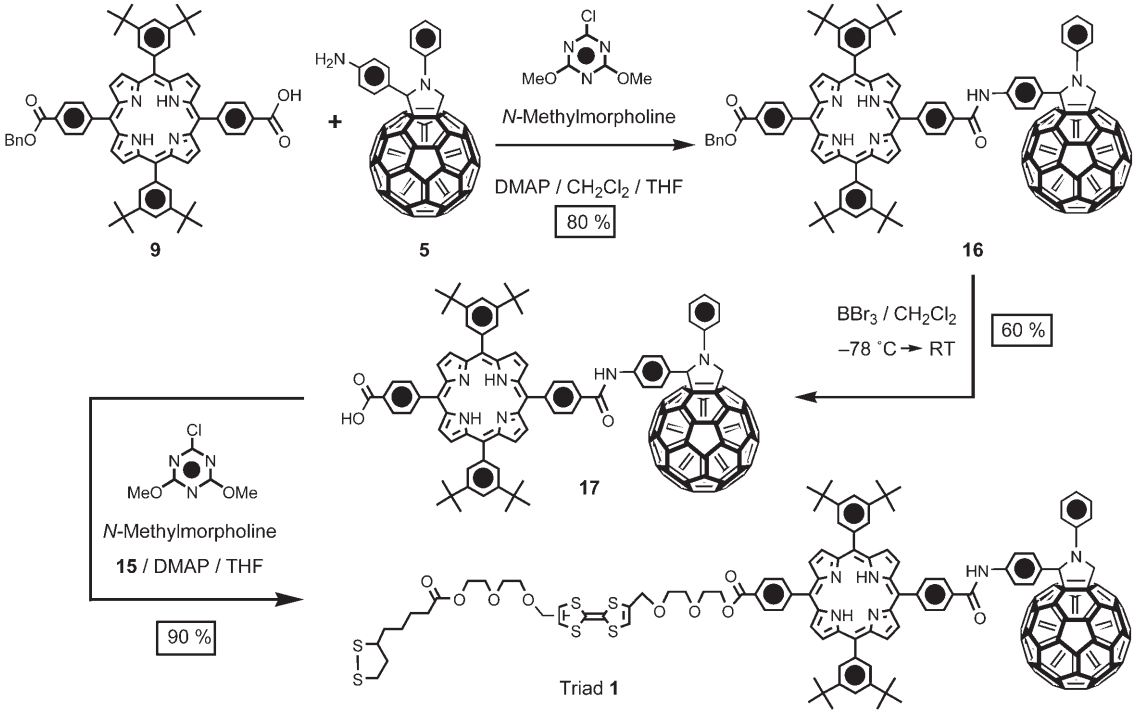

Scheme 5. The synthesis of the triad **1**.

methane for 3–5 days. The SAM-functionalized gold surfaces were characterized by cyclic voltammetry (CV). They were used subsequently as the working electrodes in the cells employed for the detailed electrochemical studies described later on in this paper.

UV-visible and photoaction spectra: The absorption spectra of the triad **1**, the P–C_{60} dyad **16** and the other building blocks are shown in Figure 2. The triad **1** in CH_2Cl_2 shows absorption features at 253, 305, 326, 420, 451, 516, 551, 590, and 646 nm. These features are a linear combination[10b,c] of the absorption bands of each of the components (building blocks) present in the molecule. The 253 nm peak is attributed to a C_{60} absorption, while those at 305 and 326 nm arise from TTF absorptions. The peaks from 420 through 646 nm are ascribed to the porphyrin's Soret and Q-bands. The linear combination[10b,c] of the absorption peaks of the C_{60}, porphyrin, and TTF units in the spectrum of **1** indicates that there is little or no electronic interaction in the ground state between any of the components present in the molecule. The absorption maximum of the porphyrin's Soret band at 420 nm is sufficiently isolated and its absorbance is much more intense than the other components. These factors can be exploited to advantage when photoexciting the porphyrin chromophore selectively into its first singlet excited state, in which it behaves like a donor.

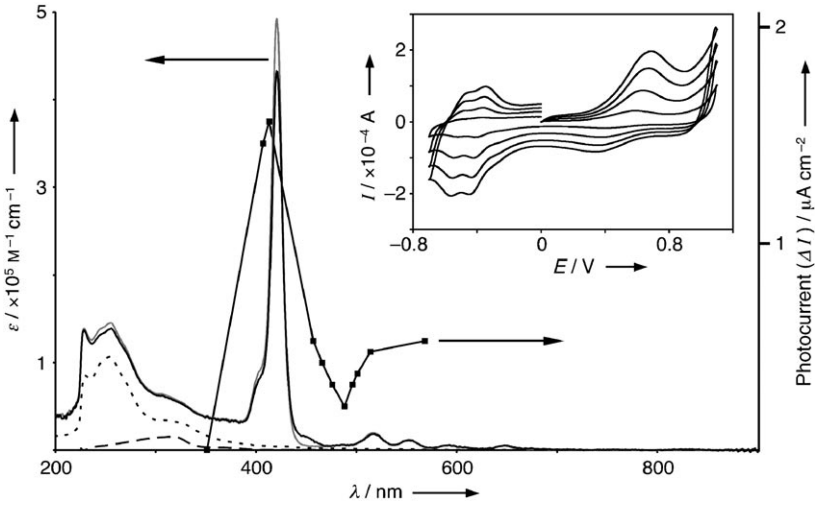

Figure 2. The photoaction spectrum (squares connected with a solid line) of a SAM of the triad **1**. The UV-visible spectra of the triad **1** (solid black line), as well as those of its building blocks, the P–C_{60} dyad (gray line), a C_{60} derivative (dotted line) and a TTF-diol (dashed line). The photoaction spectrum of the SAM of the triad **1** was collected using excitation from a Kr-ion laser and an Ar-ion laser at 34 ± 3 mW cm^{-2}. The inset displays the CV (Pt counter electrode, Ag pseudo reference electrode, 0.1 M $LiClO_4$, MeCN) of the SAM of **1** on an Au wire recorded at 100, 300, 500, and 700 mV s^{-1}—in the order of increasing peak intensity—illustrating the linear dependence of the current peak intensity with scan rate.

A photoaction spectrum is generated using a photoelectrochemical cell. It is a measure of the photocurrent that can be generated by a SAM of the triad **1** on a gold electrode when it is irradiated with various wavelengths of light. Figure 2 illustrates that the fact that the SAM of the triad **1** on a working-electrode surface generates a maximum photocurrent when the SAM is irradiated close to (413 nm) the porphyrin component's Soret band at 420 nm. In addition, photosensitization, coincident with the porphyrin component's Q-bands, is observed with excitation at 514 and 568 nm in a process that generates less photocurrent, a finding that is consistent with the smaller excitation coefficients associated with the Q-bands. Hence, in order to photoexcite the chromophoric component exclusively and to maximum effect, an excitation wavelength of 413 nm was chosen for the subsequent photochemical studies.

Electrochemistry: The redox properties of the triad **1** can be assigned (Table 1) with reference to its components and the P–C_{60} dyad **16**. The CV of each of the units displays characteristic behavior (Figure 3): the TTF-based thread is a donor that is easily oxidized[19] with two reversible, one-electron processes observed at +393 and +847 mV (versus SCE). The porphyrin is an electroactive unit that displays[9,10] both reduction and oxidation, the first of which occurs at −1176 and +1027 mV, respectively. The difference in voltage of 2203 mV between these two processes can be correlated to a visible wavelength of 563 nm, reflecting the HOMO-to-LUMO gap of the porphyrin unit, and thus correlating to the wavelengths of the Soret and Q-bands observed in the absorption spectrum. The C_{60}

Table 1. Redox potentials ($E_{1/2}$ [mV] vs SCE) of the triad **1** and its components **5**, **7**, **14**, and **16** listed going down the columns from the most positive to the most negative at 1 mM concentration in 0.1 M $TBAPF_6$/CH_2Cl_2 at room temperature.

TTF (**14**)	Porphyrin (**7**)	C_{60}-ArNH_2 (**5**)	P–C_{60} Dyad (**16**)	Triad (**1**)	Assignments
–	+1322	–	+1305[a]	–	$P^{2+/+}$
–	+1027	–	+1015	+1027	$P^{+/0}$
+847	–	–	–	+825[b]	$TTF^{2+/+}$
+393	–	–	–	+403	$TTF^{+/0}$
–	–	−658	−666	−672	$C_{60}^{0/-1}$
–	–	−1038	−1023	−1032	$C_{60}^{-1/-2}$
–	−1176	–	−1186	−1199	$P^{0/-1}$
–	−1500	–	−1551[c]	−1559[c]	$P^{-1/-2}$
–	–	−1562	−1551[c]	−1559[c]	$C_{60}^{-2/-3}$

[a] An irreversible second oxidation process of the porphyrin component in the dyad containing C_{60}. [b] A quasi-reversible second oxidation of the TTF component in the triad containing a contiguous porphyrin unit. [c] Overlapping reduction potentials.

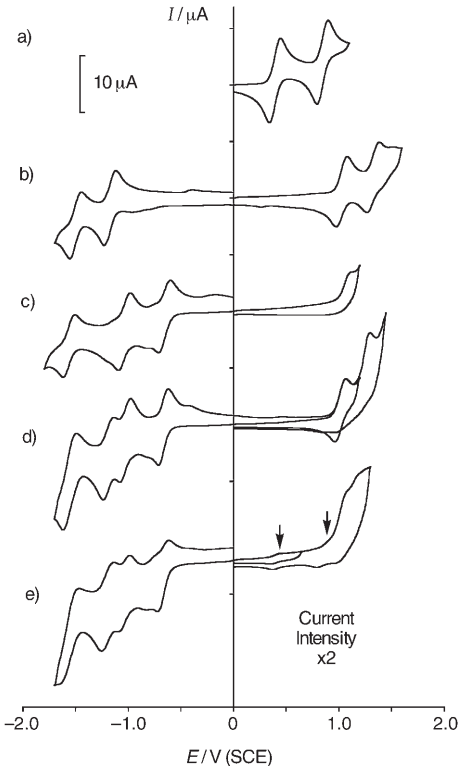

Figure 3. Cyclic voltammetry of a) TTF, b) porphyrin, c) C_{60}, d) the dyad, and e) the triad. The data were recorded as ~1 mM concentrations in 0.1 M $TBAPF_6$ solutions in CH_2Cl_2 at 200 mV s^{-1} with the standard calomel electrode (SCE) as a reference.

unit displays three one-electron quasi-reversible reductions,[9d] beginning at −658 mV, that are commensurate with its high electron-accepting ability. An irreversible oxidation process is also observed on account of a small amount of electrode adsorption of the C_{60} unit throughout the reduction region. The CV of the P–C_{60} dyad **16** is a linear combination of its component parts and each feature in the reduction region can be assigned. The process at −1551 mV is attributed to the reduction of the porphyrin component to its dianion and of the C_{60} component to its trianionic form. The dyad displays a reversible oxidation that can be assigned to the porphyrin component. A second irreversible process is observed that displays an oxidative peak at approximately +1300 mV that can be attributed to oxidation of the porphyrin component to its dication, a process occurring at a potential similar to that for the irreversible oxidation of the C_{60} component. The assignments to the CV response of the triad **1** follow a similar pattern to that of the dyad throughout the reduction region. The oxidative region, however, displays some additional features that are not straightforward to assign. In particular, the TTF component displays two oxidation features (arrows in Figure 3e) that are significantly lowered in their peak intensities, although they should be equal in magnitude with all of the other one-electron peaks. In addition, the oxidation processes assigned to the porphyrin and C_{60} components become irreversible ones in the CV of the triad. We expected that the TTF component would be involved in a charge-transfer (CT) interaction with the C_{60} component, as has been observed[9m] for various TTF–C_{60} dyads in which the two components are sufficiently close together. However, UV-visible spectra recorded at higher concentrations (1 mM) of the triad **1** did not display conclusively any characteristic band around 750 nm that could be ascribed to a TTF–C_{60} CT interaction. This lack of a TTF–C_{60} CT interaction in a triad is in the line with what Liddell et al. reported.[10b] These authors have also observed[10b] a linear combination of reversible oxidation and/or reduction peaks of all three electroactive components in the solution-phase CV investigation of their more rigid TTF–P–C_{60} triad.

The CV of the **1**-SAM on a gold wire electrode shows (Figure 2, inset) a prominent quasi-reversible[10c] peak at +680 mV, assignable to the two-electron oxidation of the TTF component. The C_{60} component displays two closely spaced reduction processes at −420 and −500 mV.[20] Assuming that the oxidation of the TTF component at +680 mV is a two-electron process, surface coverage of the triad **1** on the gold surface is estimated to be 1.4 nm^2 per molecule (1.2 mol cm^{-2}), a finding that is consistent with hexagonal close-packing of the spherical C_{60} component. It is not unlikely that the variations in the shapes of the CVs of the triad **1** in solution and it self-assembled onto a surface reflect the fact that they exist in different conformations. By contrast, the CV of SAMs of the Fc–P–C_{60} triads displayed[9c] an absence of the C_{60}-based reduction peaks, while the Fc-based oxidation peaks were readily observed. The discrepancies in the CVs of the somewhat similar types of donor–chromophore–acceptor-based triads reported in the literature[9,10] may be attributed to the differences in their detailed structure and conformational arrangements; for example, the π-electron donating units, the structure of the porphyrin units, and the distances between the components in the triad molecules are different.

Photoelectrochemistry: Photoelectrochemical experiments were carried out initially in a standard[9c] three-electrode electrochemical cell by using a gold-foil electrode functionalized with **1**-SAM as the working electrode, a platinum gauze as the counter electrode, Ag/AgCl (saturated KCl) as the reference electrode, and 0.1 M Na_2SO_4 (aqueous) as the electrolyte solution. In this particular set-up, the **1**-SAM-functionalized working electrode generated a cathodic current of ~1 μA cm^{-2} (Figure 4a) upon irradiation with a 413 nm laser light (Kr-ion laser, 34 ± 3 mW cm^{-2}), while the cell was held with a bias at −500 mV. Bare gold and decanethiol-SAM-functionalized gold electrodes did not display (Figure 4a) any light-gated response. The linear relationship (Figure 4b) of the magnitudes of the photocurrent with the laser power confirms that electronic output is a result of photon input—the larger the input of photons, the higher the output of electrons.

In a similar experiment, employing 0.1 M $TBAPF_6$ in MeCN as the electrolyte solution and Ag wire as the pseudo-reference electrode in a more compact electrochemical cell with shorter distances between the electrodes, led to

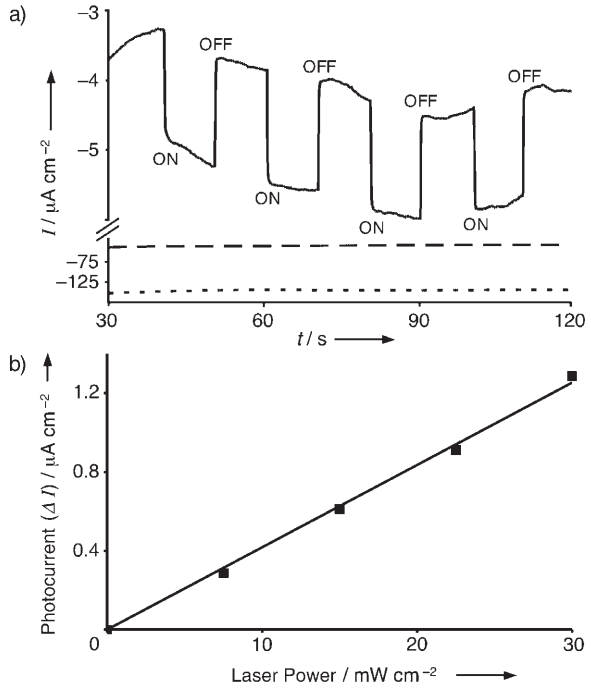

Figure 4. a) The photocurrent switching cycle (solid line) of the triad **1** in a SAM on Au, recorded in the photoelectrochemical cell by gating 413 nm excitation ON and OFF every 10 s after the current response has reached an equilibrium value with polarization at −500 mV (0.1 M Na_2SO_4, aerated). The bottom two traces were recorded under identical conditions on a SAM of decanethiol (dashed line) and on bare Au (dotted line). b) A plot illustrating the linearity of the difference between the ON and OFF signals in the photocurrent response (ΔI) with laser intensity, recorded under the same conditions as those described in a).

the generation[21] of a higher and more stable cathodic photocurrent (~1.4 $\mu A\,cm^{-2}$), even at an applied potential (E_{ap}) of 0 V. No photocurrent was observed when the applied potential was set at or above +700 mV, which is just above the oxidation potential of the TTF component in the **1**-SAM. An applied potential threshold of +650 mV for the photocurrent generation is roughly concomitant with the oxidation potential (+680 mV) of the TTF component in the **1**-SAM. This phenomenon can be attributed to the unidirectional flow of electrons from the gold-working electrode through the SAM to the platinum counter electrode through the electrolyte solution. In an open circuit, a photovoltage of −12 mV was measured in the presence of a 413 nm laser (40 $mW\,cm^{-2}$). The quantum efficiency of the photocurrent generation by the triad **1** was estimated to be ~1%, based on the photocurrent output of 1.3 $\mu A\,cm^{-2}$ arising from a 413 laser input of 26 $mW\,cm^{-2}$. In the optimized conditions, the Fc-donor-based triad was reported[9c] to show 20–25% photocurrent efficiency.

Dethreading of a pseudorotaxane: Finally, the **1**-SAM was employed (Figure 5a) as a molecular-level energy supply to power the dethreading of a [2]pseudorotaxane (BHEEN⊂$CBPQT^{4+}$) composed of a π-electron-rich BHEEN thread and a π-electron-deficient $CBPQT^{4+}$ cyclophane. The experimental set-up is illustrated in Figure 5b. The pseudorotaxane can be considered as a reasonably stable CT complex between the BHEEN thread and the $CBPQT^{4+}$ cyclophane. However, reduction[5a,21] of the $CBPQT^{4+}$ to the corresponding $CBPQT^{\bullet 3+}$ weakens the CT interaction, which, in turn, results in the decomplexation of the $CBPQT^{\bullet 3+}$ unit from the BHEEN thread. The dethreading process can be monitored by measuring the increase in the fluorescence intensity of the free BHEEN relative to the weakly fluorescent complexed BHEEN. The required electrochemical potential for the $CBPQT^{4+/\bullet 3+}$ reduction process is −300 mV. The introduction of a working electrode functionalized with the photoactive triad **1** into an electrochemical cell containing the pseudorotaxane in the electrolyte solution caused a gradual increase in the BHEEN's fluorescence intensity (Figure 5c), even at $E_{ap}=0$ V while the functionalized working electrode was being irradiated with 413 nm laser light during a period of 2900 s. The increase in the BHEEN's fluorescence intensity is also accompanied (Figure 5d) by the generation of an average photocurrent of 1.1 $\mu A\,cm^{-2}$ generated over the excitation period. However, the BHEEN-based fluorescence remained almost unaffected at 0 V when the 413 nm excitation was switched OFF, and consequently, no photocurrent was generated. Irradiation of the **1**-SAM with 413 nm light generates the charge-separated species $TTF^{\bullet+}$–P–$C_{60}^{\bullet-}$, which releases its electron from the $C_{60}^{\bullet-}$ ($E_{red}=-500$ mV) to the pseudorotaxane present in the surrounding electrolyte solution. Therefore, even at an applied potential of 0 V, and in the presence of a 413 nm laser, the effective cathodic potential at the working electrode functionalized with the triad **1** is −500 mV, a potential which is higher than the threshold of −300 mV that is required for the dethreading process.

The pseudorotaxane was dethreaded deliberately (Figure 6) in the absence of the 413 nm laser following the direct electrochemical reduction of the $CBPQT^{4+}$ cyclophane by applying a −500 mV bias for 1200 s. A time-lag of ~100 s for the increase in fluorescence intensity of the BHEEN was observed. It arises because of the diffusion of the free components from the bare gold-foil working electrode to the site of the UV excitation. A gradual increase in the fluorescence intensity, synchronized with a gradual decrease of the cathodic current, was observed until about 750 s, at which point, both of the current and fluorescence traces reached their corresponding saturation points and remained constant thereafter. An almost constant (750–1200 s) fluorescence intensity, even when the cell was biased at −500 mV, leads us to the conclusion that almost all (~100%) of the pseudorotaxane became dissociated within the first 750 s. Moreover, the observation of almost no attenuation of the fluorescence intensity within 1200–1800 s when no bias was applied indicates that the oxidation of the reduced $CBPQT^{\bullet 3+}$ to $CBPQT^{4+}$ by ambient O_2 and its subsequent reassociation with the BHEEN is an extremely slow process.

The background signal arising from the scattering of the 413 nm light was determined by comparing (Figure 7) the fluorescence intensity with the 413 nm laser ON, but with

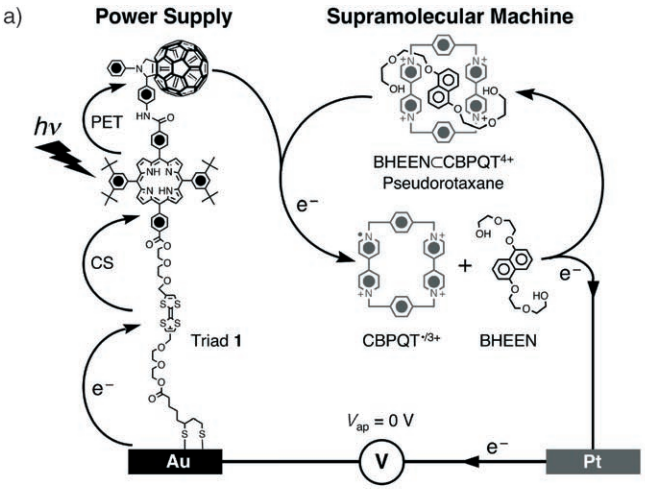

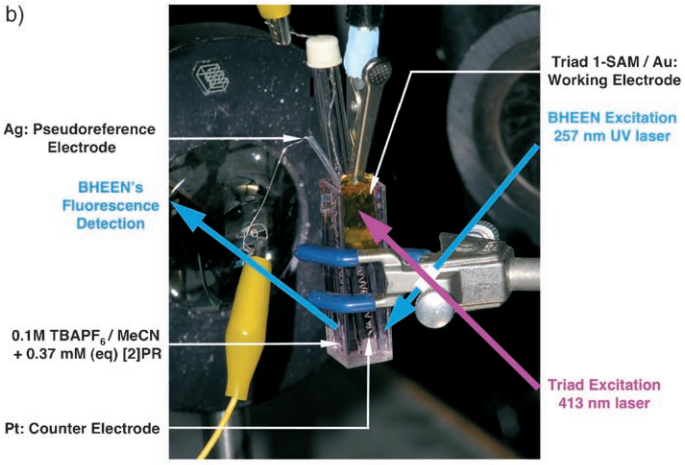

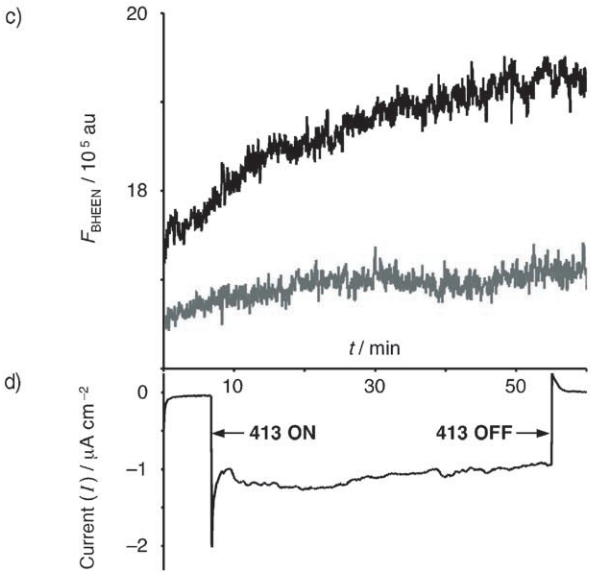

Figure 5. a) Schematic representation illustrating how the light-driven power supply, that is, the triad **1**, provides the electrical energy to dethread a [2]pseudorotaxane ([2]PR) wherein BHEEN is encapsulated inside the cavity of a $CBPQT^{4+}$ cyclophane. The curved arrows indicate the vectorial electron transfer (PET) from the photo-excited porphyrin chromophore to the C_{60} component, followed by a charge shift (CS) to the TTF component, and finally a charge neutralization by the Au electrode in a closed circuit. Subsequently, the electron is transferred to the pseudorotaxane, leading to dethreading of the reduced $CBPQT^{\bullet/3+}$ before its electron is passed onto the Pt counter electrode. b) Experimental set-up for the dethreading experiment; the colored arrows indicate the excitation and emission pathways of the respective units. c) The dethreading process synchronized with a photocurrent generation at an applied potential of 0 V monitored by the increase in BHEEN's florescence (top trace) with excitation at 257 nm. The fluorescence (bottom trace) of the BHEEN unit in the absence of porphyrin excitation. d) The photocurrent generation as a result of the photoexcitation by 413 nm laser.

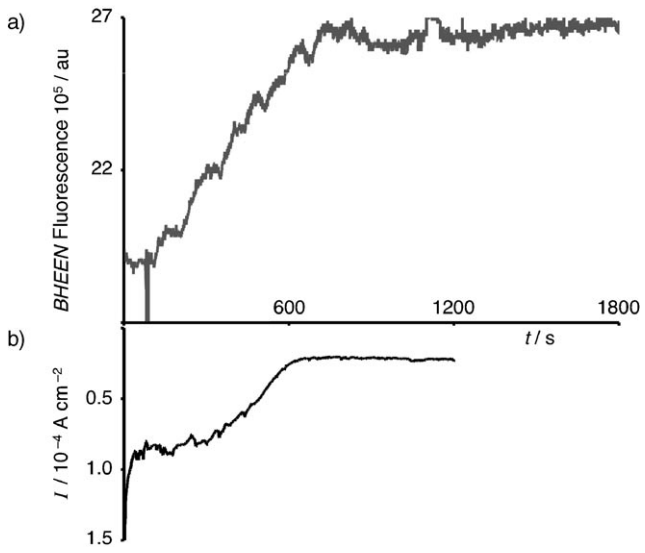

Figure 6. a) Fluorescence of BHEEN when the $CBPQT^{4+}$ cyclophane is directly reduced at −500 mV. The observed plateau for the trace after 750 s, even when the cell is biased at −500 mV for 1200 s indicates complete dethreading after 750 s. b) Current versus time plot at −500 mV.

the BHEEN excitation (UV) turned ON and then OFF. With the 413 nm laser ON, while the UV was ON or OFF, no significant signal for the 413 nm irradiation was detected by the fluorescence detector.

A simple calculation verifies that the percent increase in the fluorescence intensity is consistent with the percent dissociation of the total pseudorotaxane by the photocurrent. At −500 mV, an average current of 6.12×10^{-5} A for 750 s, which generates 4.7×10^{-7} mol of electrons, causes complete (~100%) dissociation of the pseudorotaxane, as shown by the saturation of the fluorescence intensity after 750 s. Consequently, at 0 V, an average photocurrent of 1.1 μA for 2900 s, which generates 3.3×10^{-8} mol of electrons, should be able to dethread 7% of the pseudorotaxane. In the same experiment at 0 V, the BHEEN's fluorescence intensity increased[23] by 6.7% with respect to its initial intensity; an ob-

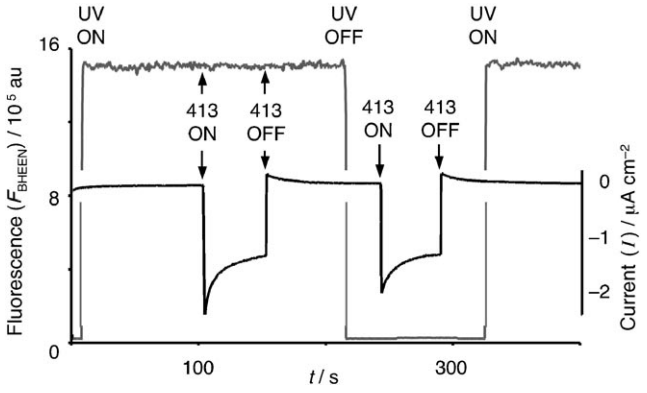

Figure 7. Background correction for the effect of the 413 nm laser scattering on the BHEEN-based fluorescence intensity. Note that there is almost no change in the fluorescence intensity (grey trace) concomitant with the photocurrent generation (black trace) by the 413 nm laser, both when UV excitation of BHEEN is kept ON and kept OFF.

servation that is consistent with the percent increase in the free BHEEN concentration, estimated based on the electron-count. The decomplexation of the pseudorotaxane by the photosensitization of the light-harvesting molecular triad **1** at an applied potential of 0 V is therefore a direct result of the photoreduction of the electron-acceptor C_{60} component, which passes its electron onto the pseudotottaxanes present in the adjacent electrolyte solution, causing the electrochemical reduction of the $CBPQT^{4+}$ cyclophane, resulting in its dethreading from the BHEEN in a chain process that can be controlled by a specific wavelength of laser light. Thus, we have demonstrated how the actuation of the two parts of a pseudorotaxane can be controlled using light energy by simply introducing a photoactive molecule into an appropriate supramolecular environment.

Conclusion

A variety of donor–chromophore–acceptor-based light-harvesting molecular dyads and triads have already been applied[9–13] in several different ways, such as 1) inducing active transport on ions across artificial lipid membranes, 2) converting light to electrical energy, and 3) powering nanoscale machinery. These dyads and triads may be optimized into a true photocell,[24] generating photovoltages that are proportional to the light power. Moreover, their uses may be extended even further by utilizing them as nanoscale power supplies in appropriate environments to drive and control molecular and supramolecular actuations. Their functions as power supplies can, in turn, be regulated exclusively by nature's most universal and abundant energy source—light. In this piece of work, we have demonstrated how a molecular triad can be employed as a power supply for a supramolecular machine. Clearly, if this molecular triad can be integrated into a bistable [2]rotaxane, we would have a photodriven molecular machine based on a light-harvesting system at the nanoscale level.

Experimental Section

General methods: Starting materials and reagents were purchased from Aldrich and used as received. The *N*-boc-4-aminobenzaldehyde derivative **3** and compounds **10**–**14** were prepared as described in the literature.[15,17,18] All reactions were performed under an argon atmosphere and in dry solvents unless otherwise noted. Analytical TLC was performed on silica gel 60-F_{254} (Merck) with detection by fluorescence and/or by developing in an iodine chamber. Flash chromatography was performed with silica gel 60 (Silicycle). The TTF derivative **15**, the P–C_{60} dyads **16** and **17**, and the triad **1** are all mixtures of several diastereoisomers. No attempt was made to isolate them. ^{1}H NMR spectra were recorded on Bruker ARX 400 MHz, Bruker Avance 500 MHz, or Bruker Avance 600 MHz spectrometers at ambient temperature in appropriate deuterated solvents using tetramethylsilane as an internal reference. High-resolution matrix-assisted laser desorption ionization mass spectra (HR-MALDI-MS) were recorded on an IonSpec Ultima 7.0T FT-ICR MALDI mass spectrometer with dihydroxybenzoic acid (DHB), α-cyano-hydroxycinnamic acid (α-CN), or terthiophene as a matrix and A19L oligopeptide (APPPDPDPGP EIKAKRLNL, monoisotopic mass = 2024.1) as an external calibration.

Compound 4: This compound was prepared by using a slight modification of the literature procedure.[16] A homogeneous solution of C_{60} (1.44 g, 2 mmol), *N*-phenylglycine **2** (3.18 g, 20 mmol), and the benzaldehyde derivative **3**[15] (440 mg, 2 mmol) in 1,2-dichlorobenzene (300 mL) was heated under reflux for 1.5 h. After cooling down to room temperature, the reaction mixture was subjected to silica gel (SiO_2) column chromatography, eluting first with hexanes and then with PhMe to obtain the C_{60} adduct **4** (820 mg, 40% yield) as a brown solid. ^{1}H NMR (500 MHz, $CDCl_3$): $\delta = 1.41$ (s, 9H), 4.90 (d, $J = 10$ Hz, 1H), 5.58 (d, $J = 10$ Hz, 1H), 5.96 (s, 1H), 6.36 (s, 1H), 7.10 (d, $J = 9$ Hz, 2H), 7.27–7.29 (m, 5H), 7.64 ppm (d, $J = 9$ Hz, 2H); MS (MALDI-TOF): m/z: 1030.7 $[M+H]^+$ (DHB matrix).

Compound 5: A solution of **4** (1.6 g, 1.5 mmol) and trifluoroacetic acid (40 mL) in PhMe (300 mL) was heated under reflux for 3 h. After cooling down the reaction mixture, the solvent was removed, and the residue was re-dissolved in PhMe (50 mL). The remaining acid was quenched with Et_3N (20 mL). The solvents were then evaporated off and the residual solid was re-dissolved in a minimum volume of PhMe. Column chromatography (SiO_2: PhMe) afforded the free amine **5** (1.3 g, 90% yield) as a dark brown solid. ^{1}H NMR (600 MHz, $CDCl_3$): $\delta = 4.89$ (d, $J = 10$ Hz, 1H), 5.57 (d, $J = 10$ Hz, 1H), 5.90 (s, 1H), 6.57 (d, $J = 8$ Hz, 2H), 7.27–7.30 (m, 5H), 7.49 ppm (d, $J = 8$ Hz, 2H); MS (HR-MALDI): m/z: 929.2163 $[M+H]^+$ (DHB matrix).

Compound 6: This compound was prepared by using a slight modification of the literature procedure.[16] A solution of methyl-4-formylbenzoate (17.25 g, 105.1 mmol) in pyrrole (75 mL, 1.06 mol) was degassed by bubbling Ar for 2 h. After adding trifluoroacetic acid (0.21 mL, 2.8 mmol) to the degassed solution, it was stirred at 20 °C in the dark for 4 h. The reaction mixture was diluted with C_6H_6 (200 mL) and washed with 0.1 M aqueous NaOH solution and H_2O successively. The organic layer was dried (Na_2SO_4), and the solvent and the excess of pyrrole were removed under reduced pressure to afford a viscous brown oil, which was then coated on SiO_2 (20 mL) and purified by flash column chromatography (SiO_2: C_6H_6/EtOAc/Et_3N 100:2.5:1.0 to 100:5.0:1.0). The first pale yellow fraction was collected and the solvent was removed under reduced pressure at room temperature. The resulting solid was washed with cold EtOAc (50 mL) and a subsequent filtration afforded **6** (13.3 g, 42% yield) as a beige crystalline solid. ^{1}H NMR (400 MHz, $CDCl_3$): $\delta = 3.80$ (s, 3H), 5.42 (s, 1H), 5.79 (s, 2H), 6.06 (d, $J = 3$ Hz, 2H), 6.61 (d, $J = 1$ Hz, 2H), 7.17 (t, $J = 7$ Hz, 2H), 7.86 ppm (d, $J = 8$ Hz, 4H).

Compound 7: This compound was prepared by using a slight modification of the literature procedure.[16] A solution of **6** (13.30 g, 47 mmol) and 3,5-di-*tert*-butylbenzaldehyde (10.36 g, 47 mmol) in $CHCl_3$ (4 L) was degassed by bubbling Ar for 2 h. Following addition of $BF_3{\cdot}Et_2O$ (6.02 mL, 47 mmol) to the degassed solution, it was stirred at 20 °C in the dark for 2 h. Subsequently, *p*-chloranil (18 g, 76 mmol) was added to the resulting dark red solution. After stirring for another 12 h, Et_3N (20 mL,

150 mmol) was added to the reaction mixture to neutralize the Lewis acid. The reaction mixture was then concentrated. Flash column chromatography (SiO_2: $CHCl_3$) of the crude reaction mixture, followed by the washing of the resulting purple solid with cold MeOH (50 mL) provided **7** as the major product in a mixture of three different porphyrins. Further column chromatography (SiO_2: hexanes/PhMe 2:1 to 1:3) afforded the desired *meso*-porphyrin **7** as the second fraction. Evaporation of the solvent from this fraction yielded a purple solid (3.6 g, 14% yield). ^{1}H NMR (600 MHz, $CDCl_3$): $\delta = -2.74$ (s, 2H), 1.54 (s, 36H), 4.12 (s, 6H), 7.81 (d, $J = 2$ Hz, 2H), 8.07 (s, 4H), 8.31 (d, $J = 8$ Hz, 4H), 8.43 (d, $J = 8$ Hz, 4H), 8.79 (d, $J = 5$ Hz, 4H), 8.90 ppm (d, $J = 5$ Hz, 4H).

Compound 8: This compound was prepared by using a slight modification of the literature procedure.[16] A solution of **7** (1.01 g, 1.05 mmol) in a THF/EtOH mixture (1/1, 500 mL) and KOH (5.4 g) in H_2O (50 mL) was heated under reflux for 12 h. After cooling, the organic solvent was removed under reduced pressure and the residue was diluted with H_2O (200 mL). The resulting dipotassium salt of the corresponding porphyrin dicarboxylic acid was then filtered off. An acidification of the solid dipotassium salt with conc. HCl, followed by thorough washing of the residue with hot H_2O provided the dicarboxylic acid **8** (950 mg, 97% yield) as a purple powder. ^{1}H NMR (500 MHz, $CDCl_3$/$(CD_3)_2SO$ 3:1): $\delta = -3.62$ (brs, 2H), 1.78 (s, 36H), 7.03 (brs, 2H), 7.26 (brs, 4H), 7.52 (m, 4H), 7.64 (m, 4H), 8.05 (brs, 4H), 8.12 ppm (brs, 4H).

Compound 9: 4-Methylmorpholine (1 mL, excess) was added to a solution of **8** (927 mg, 1 mmol) in THF (300 mL) and the reaction mixture was stirred at 20°C for 10 min. Then, 2-chloro-4,6-dimethoxy-1,3,5-triazine (386 mg, 2.2 mmol) was added to it at 0°C. The resulting solution was stirred at 0°C for 10 min and then at 20°C for 4 h. TLC of this solution showed the appearance of a less polar compound (the activated ester) at the expense of dicarboxylic acid **8**. Subsequently, a solution of benzyl alcohol (103 μL, 1 mmol) and 4-dimethylaminopyridine (200 mg) in THF (100 mL) was added dropwise into the solution of the activated ester. The resulting reaction mixture was then stirred at 20°C for 10 h. After an aqueous workup and extraction with a $CHCl_3$/MeOH mixture (3×100 mL, 4:1), the combined organic solution was dried (Na_2SO_4) and evaporated under reduced pressure. The desired monoester **9** was isolated by flash column chromatography (SiO_2: $CHCl_3$/MeOH 98:2 to 95:5) as the second fraction. Evaporation of solvent from this fraction afforded **9** (610 mg, 60% yield) as a purple powder. ^{1}H NMR (600 MHz, $CDCl_3$): $\delta = -2.73$ (brs, 2H), 1.54 (s, 36H), 5.56 (s, 2H), 7.42 (d, $J = 8$ Hz, 2H), 7.47 (t, $J = 8$ Hz, 2H), 7.60 (d, $J = 8$ Hz, 2H), 7.81 (brs, 2H), 8.08 (s, 4H), 8.32 (d, $J = 8$ Hz, 2H), 8.35 (d, $J = 8$ Hz, 2H), 8.47 (d, $J = 8$ Hz, 2H), 8.51 (d, $J = 8$ Hz, 2H), 8.80 (d, $J = 5$ Hz, 4H), 8.92 ppm (t, $J = 5$ Hz, 4H); MS (HR-MALDI): m/z: 1017.5312 $[M+H]^+$ (DHB matrix).

Compound 15: 4-Methylmorpholine (0.2 mL, 1.6 mmol) was added to a solution of thioctic acid (206 mg, 1 mmol) in CH_2Cl_2 (50 mL) and the resulting solution was stirred at 20°C for 10 min. Then, 2-chloro-4,6-dimethoxy-1,3,5-triazine (193 mg, 1.1 mmol) was added to the reaction mixture at 0°C. The resulting solution was stirred at 0°C for 10 min and then at 20°C for 3 h. Subsequently, a solution of **14**[17,18] (440 mg, 1 mmol) and 4-dimethylaminopyridine (100 mg) in CH_2Cl_2 (20 mL) was added to the solution of the activated ester in one portion. The resulting reaction mixture was stirred at 20°C for 4 h. The solvent was then removed under reduced pressure and the crude reaction mixture was coated on neutral alumina. The ester **15** (250 mg, 40% yield) was purified by gradient column chromatography (SiO_2: CH_2Cl_2/hexanes 90:10 to CH_2Cl_2/MeOH 97:3) and was isolated as a yellow oil. ^{1}H NMR (500 MHz, $(CD_3)_2CO$): $\delta =$ 1.46–1.50 (m, 2H), 1.61–1.66 (m, 4H), 1.70–1.75 (m, 1H), 1.87–1.95 (m, 1H), 2.33 (t, $J = 8$ Hz, 2H), 2.45–2.51 (m, 1H), 3.09–3.13 (m, 1H), 3.18–3.21 (m, 1H), 3.50–3.54 (m, 2H), 3.58–3.64 (m, 12H), 3.65–3.67 (m, 2H), 4.18 (t, $J = 3$ Hz, 2H), 4.33 (s, 4H), 6.56 ppm (s, 2H); MS (HR-MALDI): m/z: 628.0789 $[M]^+$ (DHB matrix).

Compound 16: 4-Methylmorpholine (0.5 mL, excess) was added to a solution of **9** (765 mg, 752 μmol) in THF/ CH_2Cl_2 (1/3, 100 mL), and the resulting solution was stirred at 20°C for 10 min. Then, 2-chloro-4,6-dimethoxy-1,3,5-triazine (145 mg, 900 μmol) was added to the reaction mixture at 0°C. The resulting solution was stirred at 0°C for 10 min and then at 20°C for 3 h. TLC of this solution showed the appearance of a less polar component (activated ester) at the expense of **9**. Subsequently, a solution of the amine-appended C_{60}-adduct **5** (700 mg, 750 μmol) and 4-dimethylaminopyridine (100 mg) in CH_2Cl_2 (100 mL) was added to the reaction mixture. The resulting reaction mixture was then stirred at 20°C for 4 h. Solvent was removed under a reduced pressure and the dyad **18** was purified by flash column chromatography (SiO_2: CH_2Cl_2/hexanes 90:10 to 95:5) as the second fraction. Evaporation of the solvent from the second fraction afforded **16** (1.16 g, 80% yield) as a bright purple solid. ^{1}H NMR (500 MHz, $CDCl_3$): $\delta = -2.82$ (s, 2H), 1.55 (s, 36H), 4.83 (d, $J = 10$ Hz, 1H), 5.51 (d, $J = 10$ Hz, 1H), 5.56 (s, 2H), 5.80 (s, 1H), 7.09–7.11 (m, 2H), 7.32–7.43 (m, 4H), 7.46–7.49 (m, 2H), 7.61 (d, $J = 8$ Hz, 2H), 7.75 (d, $J = 8$ Hz, 2H), 7.80 (s, 4H), 7.88 (d, $J = 8$ Hz, 2H), 8.06 (s, 4H), 8.26 (s, 2H), 8.30 (d, $J = 8$ Hz, 2H), 8.44 (d, $J = 8$ Hz, 2H), 8.77 (d, $J = 3$ Hz, 4H), 8.88–8.91 ppm (dd, $J = 11$, 4.5 Hz, 4H); MS (HR-MALDI): m/z: 1931.0035 $[M+H]^+$ (no matrix).

Compound 17: A solution of BBr_3 (2 mL, excess) in CH_2Cl_2 (100 mL) was added slowly at −78°C to a solution of **16** (1.16 g, 601 μmol) in CH_2Cl_2 (500 mL). The resulting green solution was allowed to warm up to 20°C and stirred for another 4 h. The reaction mixture was then extracted with H_2O (3×100 mL) to remove any excess of acid. The resulting purple solution was dried (Na_2SO_4) and the organic solvent was evaporated. Column chromatography (SiO_2: $CHCl_3$/MeOH 98:2 to 95:5) and subsequent evaporation of the solvent from the second fraction afforded the dyad **17** (880 mg, 80% yield) as a purple solid. ^{1}H NMR (500 MHz, $CDCl_3$/$(CD_3)_2SO$ 4:1): $\delta = -2.88$ (brs, 2H), 1.54 (s, 36H), 4.72 (d, $J = 8$ Hz, 1H), 5.40 (d, $J = 8$ Hz, 1H), 5.84 (s, 1H), 6.58 (brs, 1H), 6.93 (d, $J = 7$ Hz, 2H), 7.22 (t, $J = 6$ Hz, 1H), 7.30–7.36 (m, 4H), 7.69 (d, $J = 6$ Hz, 2H), 7.82 (s, 2H), 8.05 (s, 6H), 8.16 (d, $J = 6$ Hz, 2H), 8.29–8.32 (m, 4H), 8.44 (d, $J = 6$ Hz, 2H), 8.76 (s, 2H), 8.80 (s, 2H), 8.88 (s, 4H), 10.45 ppm (s, 1H); UV/Vis (5.43 μM solution in THF): $\lambda_{max} = 251$ (C_{60}), 418 (porphyrin Soret band), 512, 546, 588, 644 nm (porphyrin Q-bands); MS (HR-MALDI): m/z: 1840.9566 $[M+H]^+$ (terthiophene matrix).

Compound 1: 4-Methylmorpholine (0.1 mL, excess) was added to a solution of the P–C_{60} dyad **17** (92 mg, 50 μmol) in a THF/ CH_2Cl_2 mixture (20 mL, 1:2), and the resulting solution was stirred at 20°C for 10 min. Subsequently, 2-chloro-4,6-dimethoxy-1,3,5-triazine (11 mg, 60 μmol) was added to the reaction mixture at 0°C. The resulting solution was stirred at 0°C for 10 min and then at 20°C for 3 h. TLC of this solution showed the appearance of a less polar component (activated ester) at the expense of the starting material **17**. Subsequently, a solution of TTF derivative **15** (3 equiv) and 4-dimethylaminopyridine (100 mg) in CH_2Cl_2 (100 mL) was added to the reaction mixture. The resulting solution was stirred at 20°C for 4 h. After removing the solvent from the crude reaction mixture, the residue was thoroughly washed with MeOH to remove excess of **15** and other reagents to obtain the triad **1** (98 mg, 80%). It was further purified by crystallization from a CH_2Cl_2 solution to obtain a brownish-purple solid. ^{1}H NMR (500 MHz, $CDCl_3$): $\delta = -2.81$ (s, 2H), 1.58 (brs, 36H), 1.90–1.93 (m, 2H), 2.05 (s, 2H), 2.28–2.30 (m, 2H), 2.34–2.37 (m, 1H), 3.07–3.14 (m, 5H), 3.31–3.34 (m, 1H), 3.40–3.44 (m, 2H), 3.49 (s, 2H), 3.54–3.59 (m, 2H), 3.69–3.75 (m, 4H), 3.80–3.82 (m, 2H), 3.94 (s, 1H), 3.96–3.98 (m, 2H), 4.02 (brs, 1H), 4.12–4.16 (m, 1H), 4.23–4.25 (m, 1H), 4.28 (s, 1H), 4.35 (brs, 1H), 4.68 (brs, 1H), 4.81 (d, $J = 9$ Hz, 1H),[25] 5.50 (d, $J = 9$ Hz, 1H),[25] 5.90 (s, 1H),[25] 6.23 (d, $J = 5$ Hz, 2H),[25] 7.10 (t, $J = 7$ Hz, 1H), 7.31–7.37 (m, 2H), 7.38 (t, $J = 7$ Hz, 1H), 7.76 (brs, 2H), 7.81 (s, 2H), 7.86 (brs, 2H), 8.06 (s, 4H), 8.26 (s, 4H), 8.31 (brs, 2H), 8.43–8.50 (m, 3H), 8.78 (brs, 4H), 8.89 ppm (d, $J = 6$ Hz, 4H); MS (HR-MALDI): m/z: 2451.7211 $[M+H]^+$ (DHB matrix).

Self-assembled monolayer formation: The triad **1** was self-assembled on Piranha-cleaned gold wires and foils from solutions of **1** in CH_2Cl_2 (0.1 mM) in the absence of light over a period of 72 h. The resulting SAM-modified gold surfaces were cleaned by rinsing with appropriate solvents (CH_2Cl_2 and EtOH) and used as the working electrode in the electrochemical and photoelectrochemical experiments.

Physical studies: The UV-visible absorption spectra were recorded on a Varian Cary 100 Bio in CH_2Cl_2. The extinction coefficients were obtained from a single-point determination. Electrochemical experiments were carried out at room temperature in argon-purged solutions of the samples in MeCN, with a Princeton Applied Research 263 A Multipurpose instru-

ment interfaced to a PC (EG&G software). Cyclic voltammetric (CV) experiments were performed using a glassy carbon working electrode (0.018 cm^2, Cypress Systems); its surface was polished routinely with a 0.05 μm alumina-water slurry on a felt surface immediately before use. The counter electrode was a Pt wire and the reference electrode was either SCE or Ag/AgCl. Tetrabutylammonium hexafluorophosphate (0.1 M) was added as supporting electrolyte. Cyclic voltammograms were obtained at scan rates ranging from 2 to 1000 $mV\,s^{-1}$. For reversible processes, $E_{1/2}$ was calculated from an average of the cathodic and anodic cyclic voltammetric peaks. To establish the reversibility of a process, we used the criteria of 1) 60 mV between cathodic and anodic peaks and 2) close to unity ratio of the intensities of the cathodic and anodic currents. Experimental errors: potential values, ±10 mV; absorption maxima, ±2 nm. The SAM-functionalized Au electrode (Au coil, 0.5 diameter, 2.262 cm^2 working area) for the CV experiments was washed thoroughly before use by rinsing in CH_2Cl_2, then in THF, and finally in MeCN.

Phototoelectrochemical measurements: A standard three-electrode cell, consisting of Au-foil functionalized with a SAM of the triad **1**, a Pt gauze counter electrode (in the shape of a bucket), and a Ag/AgCl (saturated KCl) reference electrode were used. The Au foil was located at the center of the Pt gauze bucket (diameter ~3 cm) counter electrode. An aqueous 0.1 M Na_2SO_4 solution (aerated) was employed as the electrolyte. Single-wavelength laser light from a Krypton ion laser (Coherent, Innova 300C, 407, 413 and 568 nm) or an Argon ion laser (Coherent Innova 90C-5, 355, 457, 466, 476, 488, 496, 501 and 514 nm) was aligned and dispersed into the photoelectrochemical cell to irradiate a ~1 cm^2 area of the Au foil. All laser powers were measured at the source and were corrected for attenuation by the intervening optics. A galvanostat experiment was performed to detect the voltage (−500 mV) at which the dark current was closest to zero. The photoaction spectrum was generated by measuring the photocurrent at −500 mV after equilibration at 100 s generated by excitation at different wavelengths at a constant power (40 $mW\,cm^{-2}$). Control experiments were conducted on bare Au foil or a decanethiol (Aldrich) and butanethiol (Aldrich) SAMs coated Au electrode. In an optimized system, a triad **1**-SAM/Au working electrode, Pt wire in a fritted tube as the counter electrode, Ag wire-pseudoreference electrode, and 0.1 M $TBAPF_6$ solution in MeCN as supporting electrolyte in a $1\times1\times3$ cm^3 quartz cuvette was used as the electrochemical cell. The same laser source and power as mentioned earlier was used for photoexcitation.

Dethreading experiments: The dethreading experiments were conducted under the same conditions as the photoelectrochemistry by using solutions of the sample in MeCN with 0.1 M $TBAPF_6$ as supporting electrolyte and with an Ag wire as a pseudo-reference electrode in a 3 mL quartz cell. The initial concentration of the pseudorotaxane at equilibrium was 0.37 mM, based on a 1:1 mixture of 0.5 mM concentrations of both BHEEN and $CBPQT^{4+}$ units and their association constant[26] of $K_a = 2.53\times10^4\,M^{-1}$ (MeCN, 298 K). The detection of fluorescence from the BHEEN has been described elsewhere.[3a] Briefly, UV excitation (Ar ion laser, Innova 300C FReD, $\lambda_{ex}=257$ nm, 10 $mW\,cm^{-1-2}$) was used and the florescence was detected at 45° through a monochromator connected to an intensified CCD camera (ICCD, PI-MAX, Princeton Instruments). The florescence versus time trace was obtained by integrating the area under the spectrum from 320 to 370 nm every 0.5 s. The florescence spectra are an average of 50 spectra obtained every 0.5 s.

Acknowledgements

This research was supported by a National Science Foundation (NSF) Nanoscale Interdisciplinary Research Team (NIRT ECS-0103559) fund, an Office of Naval Research (ONR-contract number N00014–00–1–0216) grant, an NSF Equipment Grant (CHE-9974928), an NIH Shared Instrument Grant (S10RR1S9S2) and the Center for Cell Mimetic Space Exploration (CMISE)—a NASA University Research, Engineering and Technology Institute (URETI), the award number being NCC2–1364.

[1] a) D. H. Busch, N. A. Stephenson, *Coord. Chem. Rev.* **1990**, *100*, 119–154; b) J. S. Lindsey, *New J. Chem.* **1991**, *15*, 153–180; c) D. Philp, J. F. Stoddart, *Synlett* **1991**, 445–458; d) C. A. Hunter, *J. Am. Chem. Soc.* **1992**, *114*, 5303–5311; e) S. Anderson, H. L. Anderson, J. K. M. Sanders, *Acc. Chem. Res.* **1993**, *26*, 469–475; f) A. P. Bisson, F. J. Carver, C. A. Hunter, J. P. Waltho, *J. Am. Chem. Soc.* **1994**, *116*, 10292–10293; g) C. A. Hunter, *Angew. Chem.* **1995**, *107*, 1181–1183; *Angew. Chem. Int. Ed. Engl.* **1995**, *34*, 1079–1081; h) J. P. Schneider, J. W. Kelly, *Chem. Rev.* **1995**, *95*, 2169–2187; i) D. Philp, J. F. Stoddart, *Angew. Chem.* **1996**, *108*, 1242–1286; *Angew. Chem. Int. Ed. Engl.* **1996**, *35*, 1154–1196; j) A. G. Kolchinski, N. W. Alcock, R. A. Roesner, D. H. Busch, *Chem. Commun.* **1998**, 1437–1438; k) M. Fujita, *Acc. Chem. Res.* **1999**, *32*, 53–61; l) J. Rebek, Jr., *Acc. Chem. Res.* **1999**, *32*, 278–286; m) *Templated Organic Synthesis* (Eds.: F. Diederich, P. J. Stang), Wiley-VCH, Weinheim, **1999**; n) M. Nakash, Z. C. Watson, N. Feeder, S. J. Teat, J. K. M. Sanders, *Chem. Eur. J.* **2000**, *6*, 2112–2119; o) J. K. M. Sanders, *Pure Appl. Chem.* **2000**, *72*, 2265–2274; p) D. T. Bong, T. D. Clark, J. R. Granja, M. R. Ghadiri, *Angew. Chem.* **2001**, *113*, 1016–1041; *Angew. Chem. Int. Ed.* **2001**, *40*, 988–1011; q) L. J. Prins, D. N. Reinhoudt, P. Timmerman, *Angew. Chem.* **2001**, *113*, 2446–2492; *Angew. Chem. Int. Ed.* **2001**, *40*, 2382–2426; r) S. R. Seidel, P. J. Stang, *Acc. Chem. Res.* **2002**, *35*, 972–983; s) J. F. Stoddart, H.-R. Tseng, *Proc. Natl. Acad. Sci. USA* **2002**, *99*, 4797–4800; t) R. L. E. Furlan, S. Otto, J. K. M. Sanders, *Proc. Natl. Acad. Sci. USA* **2002**, *99*, 4801–4804; u) D. Joester, E. Walter, M. Losson, R. Pugin, H. P. Merkle, F. Diederich, *Angew. Chem.* **2003**, *115*, 1524–1528; *Angew. Chem. Int. Ed.* **2003**, *42*, 1486–1490; v) L. Hogg, D. A. Leigh, P. J. Lusby, A. Morelli, S. Parsons, J. K. Y. Wong, *Angew. Chem.* **2004**, *116*, 1238–1241; *Angew. Chem. Int. Ed.* **2004**, *43*, 1218–1221; w) X. Zheng, M. E. Mulcahy, D. Horinek, F. Galeotti, T. F. Magnera, J. Michl, *J. Am. Chem. Soc.* **2004**, *126*, 4540–4542.

[2] Bistable catenanes and bistable rotaxanes have been employed as switches in a range of devices and across different environments. See: a) C. P. Collier, G. Mattersteig, E. W. Wong, Y. Luo, K. Beverly, J. Sampaio, F. M. Raymo, J. F. Stoddart, J. R. Heath, *Science* **2000**, *289*, 1172–1175; b) A. R. Pease, J. O. Jeppesen, J. F. Stoddart, Y. Luo, C. P. Collier, J. R. Heath, *Acc. Chem. Res.* **2001**, *34*, 434–444; c) Y. Luo, C. P. Collier, J. O. Jeppesen, K. A. Neilsen, E. DeIonno, G. Ho, J. Perkins, H.-R. Tseng, T. Yamamoto, J. F. Stoddart, J. R. Heath, *ChemPhysChem* **2002**, *3*, 519–525; d) M. R. Diehl, D. W. Steuerman, H.-R. Tseng, S. A. Vignon, A. Star, P. C. Celestre, J. F. Stoddart, J. R. Heath, *ChemPhysChem* **2003**, *4*, 1335–1339; e) H.-R. Tseng, D. Wu, N. Fang, X. Zhang, J. F. Stoddart, *ChemPhysChem* **2004**, *5*, 111–116; f) D. W. Steuerman, H.-R. Tseng, A. J. Peters, A. H. Flood, J. O. Jeppesen, K. A. Nielsen, J. F. Stoddart, J. R. Heath, *Angew. Chem.* **2004**, *116*, 6648–6653; *Angew. Chem. Int. Ed.* **2004**, *43*, 6486–6491; g) A. H. Flood, A. J. Peters, S. A. Vignon, D. W. Steuerman, H.-R. Tseng, S. Kang, J. R. Heath, J. F. Stoddart, *Chem. Eur. J.* **2004**, *10*, 6558–6564; h) A. H. Flood, J. F. Stoddart, D. W. Steuerman, J. R. Heath, *Science* **2004**, *306*, 2055–2056; i) S. S. Jang, Y. H. Kim, W. A. Goddard III, A. H. Flood, B. W. Laursen, H.-R. Tseng, J. F. Stoddart, J. O. Jeppesen, J. W. Choi, D. W. Steuerman, E. DeIonno, J. R. Heath, *J. Am. Chem. Soc.* **2005**, *127*, 1563–1575.

[3] a) S. Chia, J. Cao, J. F. Stoddart, J. I. Zink, *Angew. Chem.* **2001**, *113*, 2513–2517; *Angew. Chem. Int. Ed.* **2001**, *40*, 2447–2451; b) K. Kim, W. S. Jeon, J.-K. Kang, J. W. Lee, S. Y. Jon, T. Kim, K. Kim, *Angew. Chem.* **2003**, *115*, 2395–2398; *Angew. Chem. Int. Ed.* **2003**, *42*, 2293–2296; c) B. Long, K. Nikitin, D. Fitzmaurice, *J. Am. Chem. Soc.* **2003**, *125*, 15490–15498; d) R. Hernandez, H.-R Tseng, J. W. Wong, J. F. Stoddart, J. I. Zink, *J. Am. Chem. Soc.* **2004**, *126*, 3370–3371; e) T. J. Huang, H.-R. Tseng, L. Sha, W. Lu, B. Brough, A. H. Flood, B.-D. Yu, P. C. Celestre, J. P. Chang, J. F. Stoddart, C.-M. Ho, *Nano Lett.* **2004**, *4*, 2065–2071; f) I. C. Lee, C. W. Frank, T. Yamamoto, H.-R. Tseng, A. H. Flood, J. F. Stoddart, J. O. Jeppesen, *Langmuir* **2004**, *20*, 5809–5818; g) T. J. Huang, B. Brough, C.-M. Ho, Y. Liu, A. H. Flood, P. A. Bonvallet, H.-R. Tseng, J. F. Stoddart, M. Baller,

S. Magonov, *Appl. Phys. Lett.* **2004**, *85*, 5391–5393; h) E. Katz, L. Sheeney-Haj-Ichia, I. Willner, *Angew. Chem.* **2004**, *116*, 3354–3362; *Angew. Chem. Int. Ed.* **2004**, *43*, 3292–3300; i) O. Lioubashevski, V. I. Chegel, F. Patolsky, E. Katz, I. Willner, *J. Am. Chem. Soc.* **2004**, *126*, 7133–7143.

[4] a) L. Raehm, J.-M. Kern, J.-P. Sauvage, C. Hamann, S. Palacin, J.-P. Bourgoin, *Chem. Eur. J.* **2002**, *8*, 2153–2162; b) N. Weber, C. Hamann, J.-M. Kern, J.-P. Sauvage, *Inorg. Chem.* **2003**, *42*, 6780–6792; c) E. Coronado, A. Forment-Aliaga, P. Gaviña, F. M. Romero, *Inorg. Chem.* **2003**, *42*, 6959–6961; d) A. L. Vance, T. M. Willey, T. van Buuren, A. J. Nelson, C. Bostedt, G. A. Fox, L. J. Terminello, *Nano Lett.* **2003**, *3*, 81–84; e) H. Azehara, W. Mizutani, Y. Suzuki, T. Ishida, Y. Nagawa, H. Tokumoto, K. Hiratani, *Langmuir* **2003**, *19*, 2115–2123; f) M. Cavallini, F. Biscarini, S. León, F. Zerbetto, G. Bottari, D. A. Leigh, *Science* **2003**, *299*, 531–531.

[5] a) R. Ballardini, V. Balzani, M. T. Gandolfi, L. Prodi, M. Venturi, D. Philp, H. G. Ricketts, J. F. Stoddart, *Angew. Chem.* **1993**, *105*, 1362–1364; *Angew. Chem. Int. Ed. Engl.* **1993**, *32*, 1301–1303; b) P. R. Ashton, R. Ballardini, V. Balzani, S. E. Boyd, A. Credi, M. T. Gandolfi, M. Gómez-López, S. Iqbal, D. Philp, J. A. Preece, L. Prodi, H. G. Ricketts, J. F. Stoddart, M. S. Tolley, M. Venturi, A. J. P. White, D. J. Williams, *Chem. Eur. J.* **1997**, *3*, 152–170.

[6] a) R. A. Bissell, E. Córdova, A. E. Kaifer, J. F. Stoddart, *Nature* **1994**, *369*, 133–137; b) P.-L. Anelli, M. Asakawa, P. R. Ashton, R. A. Bissell, G. Clavier, R. Górski, A. E. Kaifer, S. J. Langford, G. Mattersteig, S. Menzer, D. Philp, A. M. Z. Slawin, N. Spencer, J. F. Stoddart, M. S. Tolley, D. J. Williams, *Chem. Eur. J.* **1997**, *3*, 1136–1150; c) P. R. Ashton, R. Ballardini, V. Balzani, A. Credi, K. R. Dress, E. Ishow, C. J. Kleverlaan, O. Kocian, J. A. Preece, N. Spencer, J. F. Stoddart, M. Venturi, S. Wenger, *Chem. Eur. J.* **2000**, *6*, 3558–3574; d) J. O. Jeppesen, K. A. Nielsen, J. Perkins, S. A. Vignon, A. Di Fabio, R. Ballardini, M. T. Gandolfi, M. Venturi, V. Balzani, J. Becher, J. F. Stoddart, *Chem. Eur. J.* **2003**, *9*, 2982–3007; e) J. O. Jeppesen, S. A. Vignon, J. F. Stoddart, *Chem. Eur. J.* **2003**, *9*, 4611–4625; f) H.-R. Tseng, S. A. Vignon, P. C. Celestre, J. Perkins, J. O. Jeppesen, A. Di Fabio, R. Ballardini, M. T. Gandolfi, M. Venturi, V. Balzani, J. F. Stoddart, *Chem. Eur. J.* **2004**, *10*, 155–172; g) B. W. Laursen, S. Nygaard, J. O. Jeppesen, J. F. Stoddart, *Org. Lett.* **2004**, *6*, 4167–4170; h) T. Iijima, E. Apostoli, V. Balzani, J. F. Stoddart, *Chem. Eur. J.* **2004**, *10*, 6375–6392; i) J. O. Jeppesen, S. Nygaard, S. A. Vignon, J. F. Stoddart, *Eur. J. Org. Chem.* **2005**, 196–220.

[7] a) J. F. Stoddart, *Chem. Aust.* **1992**, *59*, 576–577 and 581; b) M. Gómez-López, J. A. Preece, J. F. Stoddart, *Nanotechnology* **1996**, *7*, 183–192; c) V. Balzani, M. Gómez-López, J. F. Stoddart, *Acc. Chem. Res.* **1998**, *31*, 405–414; d) V. Balzani, A. Credi, F. M. Raymo, J. F. Stoddart, *Angew. Chem.* **2000**, *112*, 3484–3530; *Angew. Chem. Int. Ed.* **2000**, *39*, 3348–3391; e) A. Harada, *Acc. Chem. Res.* **2001**, *34*, 456–464; f) C. A. Schalley, K. Beizai, F. Vögtle, *Acc. Chem. Res.* **2001**, *34*, 465–476; g) J.-P. Collin, C. Dietrich-Buchecker, P. Gaviña, M. C. Jiménez-Molero, J.-P. Sauvage, *Acc. Chem. Res.* **2001**, *34*, 477–487; h) R. Ballardini, V. Balzani, A. Credi, M. T. Gandolfi, M. Venturi, *Struct. Bonding* **2001**, *99*, 163–188; i) L. Raehm, J.-P. Sauvage, *Struct. Bonding* **2001**, *99*, 55–78; j) C. A. Stainer, S. J. Alderman, T. D. W. Claridge, H. L. Anderson, *Angew. Chem.* **2002**, *114*, 1847–1850; *Angew. Chem. Int. Ed.* **2002**, *41*, 1769–1772; k) V. Balzani, A. Credi, M. Venturi, *Chem. Eur. J.* **2002**, *8*, 5524–5532; l) H.-R. Tseng, J. F. Stoddart in *Modern Arene Chemistry* (Ed.: D. Astruc), Wiley-VCH, Weinheim, **2002**, p 574–599; m) V. Balzani, A. Credi, M. Venturi, *Molecular Devices and Machines-A Journey into the Nano World*, Wiley-VCH, Weinheim, **2003**; n) A. H. Flood, R. J. A. Ramirez, W.-Q. Deng, R. P. Muller, W. A. Goddard III, J. F. Stoddart, *Aust. J. Chem.* **2004**, *57*, 301–322.

[8] a) T. R. Kelly, H. De Silva, R. A. Silva, *Nature* **1999**, *401*, 150–152; b) N. Koumura, R. W. Zijlstra, R. A. van Delden, H. Harada, B. L. Feringa, *Nature* **1999**, *401*, 152–155; c) Y. Yokoyama, *Chem. Rev.* **2000**, *100*, 1717–1740; d) G. Berkovic, V. Krongauz, V. Weiss, *Chem. Rev.* **2000**, *100*, 1741–1754; e) B. L. Feringa, R. A. van Delden, N. Koumura, E. M. Geertsema, *Chem. Rev.* **2000**, *100*, 1789–1816; f) T. R. Kelly, *Acc. Chem. Res.* **2001**, *34*, 514–522; g) S. Shinkai, M. Ikeda, A. Sugasaki, M. Takeuchi, *Acc. Chem. Res.* **2001**, *34*, 494–503; h) K. Oh, K.-S. Jeong, J. S. Moore, *Nature* **2001**, *414*, 889–893; i) N. Koumura, E. M. Geertsema, M. B. van Gelder, A. Meetsma, B. L. Feringa, *J. Am. Chem. Soc.* **2002**, *124*, 5037–5051; j) F. Hawthorne, J. I. Zink, J. M. Skelton, M. J. Bayer, C. Liu, E. Livshits, R. Baer, D. Neuhauser, *Science* **2004**, *303*, 1849–1851; k) J. J. D. de Jong, L. N. Lucas, R. M. Kellogg, J. H. van Esch, B. L. Feringa, *Science* **2004**, *304*, 278–281.

[9] a) M. Fujitsuka, O. Ito, H. Imahori, K. Yamada, H. Yamada, Y. Sakata, *Chem. Lett.* **1999**, 721–722; b) H. Imahori, H. Yamada, S. Ozawa, Y. Sakata, K. Ushida, *Chem. Commun.* **1999**, *13*, 1165–1166; c) H. Imahori, H. Yamada, Y. Nishimura, I. Yamazaki, Y. Sakata, *J. Phys. Chem. B* **2000**, *104*, 2099–2108; d) D. M. Guldi, *Chem. Commun.* **2000**, 321–327; e) M. Á. Herranz, B. Illescas, N. Martín, C. Luo, D. M. Guldi, *J. Org. Chem.* **2000**, *65*, 5728–5738; f) N. Martín, L. Sánchez, M. Á. Herranz, D. M. Guldi, *J. Phys. Chem. A* **2000**, *104*, 4648–4657; g) H. Li, J. O. Jeppesen; E. Levillain, J. Becher, *Chem. Commun.* **2003**, *7*, 846–847; h) L. Sánchez, I. Perez, N. Martín, D. M. Guldi, *Chem. Eur. J.* **2003**, *9*, 2457–2468; i) D. M. Guldi, C, Luo, A. Swartz, R. Gomez, J. L. Segura, N. Martín, *J. Phys. Chem. A* **2004**, *108*, 455–467; j) H. Imahori, Y. Mori, Y. Matano, *J. Photochem. Photobiol. C* **2004**, *4*, 51–83; k) H. Imahori, M. Kimura, K. Hosomizu, S. Fukuzumi, *J. Photochem. Photobiol. A* **2004**, *166*, 57–62; l) D. M. Guldi, H. Imahori, K. Tamaki, Y. Kashiwagi, H. Yamada, Y. Sakata, S. Fukuzumi, *J. Phys. Chem. A* **2004**, *108*, 541–548; m) H. Nishikawa, S. Kojima, T. Kodama, I. Ikemoto, S. Suzuki, K. Kikuchi, M. Fujitsuka, H. Luo, Y. Araki, O. Ito, *J. Phys. Chem. A* **2004**, *108*, 1881–1890; n) N. Martin, G, Francesco, J. L. Segura, D. M. Guldi, *Synth. Met.* **2004**, *147*, 57–61; o) D. M. Guldi, I Zilbermann, G. Anderson, N. A. Kotov, N. Tagmatarchis, M. Prato, *J. Mater. Chem.* **2005**, *15*, 114–118; p) J. L. Segura, N. Martin, D. M. Guldi, *Chem. Soc. Rev.* **2005**, *34*, 31–47; q) N. Martin, G, Francesco, J. L. Segura, D. M. Guldi, *Synth. Met.* **2005**, *149*, 95–96; r) G. de la Torre, F. Giacalone, J. L. Segura, N. Martín, D. M. Guldi, *Chem. Eur. J.* **2005**, *11*, 1267–1280; s) D. M. Guldi, G. M. A. Rahman, M. Prato, N. Jux, S. Qin, F. W. Shuhui, *Angew. Chem.* **2005**, *117*, 2051–2054; *Angew. Chem. Int. Ed.* **2005**, *44*, 2015–2018; t) R. S. Iglesias, C. G. Claessens, T. Torres, G. M. A. Rahman, D. M. Guldi, *Chem. Commun.* **2005**, 2113–2115.

[10] a) D. Gust, T. A. Moore, A. L. Moore, *IEEE Eng. Med. Biol.* **1994**, *13*, 58–66; b) P. A. Liddell, G. Kodis, L. Garza, J. L. Bahr, A. L. Moore, T. A. Moore, D. Gust, *Helv. Chim. Acta* **2001**, *84*, 2765–2783; c) G. Kodis, P. A. Liddell, L. Garza, A. L. Moore, T. A. Moore, D. Gust, *J. Mater. Chem.* **2002**, *12*, 2100–2108; d) G. Kodis, P. A. Liddell, A. L. Moore, T. A. Moore, D. Gust, *J. Phys. Org. Chem.* **2004**, *17*, 724–734; e) P. A. Liddell, G. Kodis, J. Andréasson, L. Garza, S. Bandyopadhyay, R. H. Mitchell, T. A. Moore, A. L. Moore, D. Gust, *J. Am. Chem. Soc.* **2004**, *126*, 4803–4811; f) P. A. Liddell, G. Kodis, D. Kuciauskas, J. Andréasson, A. L. Moore, T. A. Moore, D. Gust, *Phys. Chem. Chem. Phys.* **2004**, *6*, 5509–5515; g) S. D. Straight, J. Andréasson, G. Kodis, A. L. Moore, T. A. Moore, D. Gust, *J. Am. Chem. Soc.* **2005**, *127*, 2717–2724.

[11] a) G. Steinberg-Yfrach, P. A. Liddell, S.-C. Hung, A. L. Moore, D. Gust, T. A. Moore, *Nature* **1997**, *385*, 239–241; b) G. Steinberg-Yfrach, J.-L. Rigaud, E. N. Durantini, A. L. Moore, D. Gust, T. A. Moore, *Nature* **1998**, *392*, 479–482; c) D. Gust, T. A. Moore, A. L. Moore, *Acc. Chem. Res.* **2001**, *34*, 40–48; d) I. M. Bennett, H. M. V. Farfano, F. Bogani, A. Primak, P. A. Liddell, L. Otero, L. Sereno, J. J. Silber, A. L. Moore, T. A. Moore, D. Gust, *Nature* **2002**, *420*, 398–401.

[12] D. Kuciauskas, P. A. Liddell, S. Lin, T. E. Johnson, S. J. Weghorn, J. S. Lindsey, A. L. Moore, T. A. Moore, D. Gust, *J. Am. Chem. Soc.* **1999**, *121*, 8604–8614.

[13] For a preliminary discussion of this work see: S. Saha, L. E. Johansson, A. H. Flood, H.-R. Tseng, J. I. Zink, J. F. Stoddart, *Small* **2005**, *1*, 87–90.

[14] R. Fong II, D. I. Schuster, H. Mi, S. R. Wilson, A. U. Khan, *Proc. Electrochem. Soc.* **1998**, *98*, 262–266.

[15] T. Niimi, M. Orita, M. Okazawa-Igarashi, S. Miwa, K. Hitoshi, K, Kikuchi, E. Ball, A. Ichkawa, Y. Yamagiwa, S. Sakamoto, A. Tanaka, S. Tsukamoto, S. Fujita, K. Tatsuta, Y. Meada, K. Chikauchi, *J. Med. Chem.* **2001**, *44*, 4737–4740.
[16] C. Luo, D. M. Guldi, H. Imahori, K. Tamaki, Y. Sakata, *J. Am. Chem. Soc.* **2000**, *122*, 6535–6551.
[17] R. Andreu, J. Garín, J. Orduna, M. Savíron, J. Cousseau, A. Gorgues, V. Morisson, T. Nozdryn, J. Becher, R. P. Clausen, M. R. Bryce, P. J. Skabara, W. Dehaen, *Tetrahedron Lett.* **1994**, *35*, 9243–9246.
[18] J. G. Hansen, K. S. Bang, N. Thorup, J. Becher, *Eur. J. Org. Chem.* **2000**, *11*, 2135–2144.
[19] a) M. Asakawa, P. R. Ashton, V. Balzani, A. Credi, C. Hamers, G. Mattersteig, M. Montalti, A. N. Shipway, N. Spencer, J. F. Stoddart, M. S. Tolley, M. Venturi, A. J. P. White, and D. J. Williams, *Angew. Chem.* **1998**, *110*, 357–361; *Angew. Chem. Int. Ed.* **1998**, *37*, 333–337; b) R. Ballardini, V. Balzani, J. Becher, A. Di Fabio, M. T. Gandolfi, G. Mattersteig, M. B. Nielsen, F. M. Raymo, S. J. Rowan, J. F. Stoddart, A. J. P. White, and D. J. Williams, *J. Org. Chem.* **2000**, *65*, 4120–4126.
[20] Our observation of the reversible reductions of the C_{60} unit in the triad SAM is unique compared with the irreversible reduction of the C_{60} unit observed in the CV of a Fc–P–C_{60} triad SAM reported by Imahori (see reference[9c]). However, Kodis (see reference[10c]) has reported the observation of the first reduction of the C_{60} unit at −560 mV in a solution-phase CV of a TTF–P–C_{60} based triad.
[21] Z. M. Liu, A. A. Yasseri, J. S. Lindsey, D. F. Bocian, *Science* **2003**, *302*, 1543–1545.
[22] On average, the cyclophane is assumed to be monoreduced, on account of the 100-fold excess of the pseudorotaxane (bulk concentration 0.5 mM) compared to the dethreaded $CBPQT^{2\bullet/2+}$ cyclophane (photogenerated concentration ~5 μM) within the 3 mL of the reaction vessel. See also Figure 8a in R. Ballardini, V. Balzani, A. Credi, M. T. Gandolfi, M. Venturi, *Acc. Chem. Res.* **2001**, *34*, 445–455.
[23] Based on the electron counts in the photo-induced dethreading (E_{ap} = 0 V) and direct electrochemical dethreading (E_{ap} = −500 mV) experiments, the photocurrent generated by the triad **1** should be able to dethread only 7% of the pseudorotaxane, a change that is consistent with the fluorescence increase (6.7%) in the former case. However, when the change in the BHEEN based fluorescence intensity in the photochemical experiment was compared with that in the direct dethreading experiment, the relative fluorescence increase was found to be 16%. However, the number of electrons generated from the photocurrent would not be sufficient to dethread 16% of the pseudorotaxane. Slightly different starting fluorescence intensities in the separate experiments make it challenging to compare ΔF values from different experiments.
[24] N. Hirata, J.-J. Lagref, E. J. Palomares, J. R. Durrant, M. K. Nazeeruddin, M. Gratzel, D. Di Censo, *Chem. Eur. J.* **2004**, *10*, 595–602.
[25] Out of a total count of 108 protons present in the triad **1**, 103 of them can be accounted for based on the ^{1}H NMR integration. Characteristic chemical shifts and splitting patterns are exhibited by the protons on the fused pyrrolidine ring (3H) on the C_{60} unit and on the TTF ring (2H). Their integrated intensity, however, does not correlate perfectly on account of the shielding effect of the C_{60} unit and also, because of the complexity of the triad constitution, which generates a number of diastereoisomers.
[26] R. Castro, K. R. Nixon, J. D. Evanseck, A. E. Kaifer, *J. Org. Chem.* **1996**, *61*, 7298–7303.

Received: April 3, 2005
Published online: August 5, 2005

